THE JOURNAL OF BIOLOGICAL CHEMISTRY VOL. 291, NO. 7, pp. 3569–3580, February 12, 2016

Molecular Determinants of Kv1.3 Potassium Channels-induced Proliferation*

Received for publication, July 15, 2015, and in revised form, November 30, 2015 Published, JBC Papers in Press, December 10, 2015, DOI 10.1074/jbc.M115.678995

Laura Jiménez-Pérez[1,2], Pilar Cidad[1], Inés Álvarez-Miguel[3], Alba Santos-Hipólito, Rebeca Torres-Merino[4], Esperanza Alonso, Miguel Ángel de la Fuente, José Ramón López-López[5], and M. Teresa Pérez-García[5,6]

From the Departamento de Bioquímica y Biología Molecular y Fisiología e Instituto de Biología y Genética Molecular (IBGM), Universidad de Valladolid y Consejo Superior de Investigaciones Científicas (CSIC), 47003 Valladolid, Spain

Changes in voltage-dependent potassium channels (Kv channels) associate to proliferation in many cell types, including transfected HEK293 cells. In this system Kv1.5 overexpression decreases proliferation, whereas Kv1.3 expression increases it independently of K^+ fluxes. To identify Kv1.3 domains involved in a proliferation-associated signaling mechanism(s), we constructed chimeric Kv1.3-Kv1.5 channels and point-mutant Kv1.3 channels, which were expressed as GFP- or cherry-fusion proteins. We studied their trafficking and functional expression, combining immunocytochemical and electrophysiological methods, and their impact on cell proliferation. We found that the C terminus is necessary for Kv1.3-induced proliferation. We distinguished two residues (Tyr-447 and Ser-459) whose mutation to alanine abolished proliferation. The insertion into Kv1.5 of a sequence comprising these two residues increased proliferation rate. Moreover, Kv1.3 voltage-dependent transitions from closed to open conformation induced MEK-ERK1/2-dependent Tyr-447 phosphorylation. We conclude that the mechanisms for Kv1.3-induced proliferation involve the accessibility of key docking sites at the C terminus. For one of these sites (Tyr-447) we demonstrated the contribution of MEK/ERK-dependent phosphorylation, which is regulated by voltage-induced conformational changes.

Voltage-gated K channels (Kv)[7] comprise a large family of channels that are expressed in both excitable and non-excitable cells. In excitable cells they contribute to the control of resting membrane potential (resting E_M) and action potentials frequency and duration. In non-excitable tissues they are involved in processes ranging from secretion to cell proliferation (1–3) by means of their ability to sense and modulate E_M. Each Kv channel gene encodes a single protein, and functional Kv channels consist on homo- or heterotretrameric complexes within the same subfamily members (Kv1–Kv12). The large number of Kv channel genes combined with the possibility of heterotetramerization creates a large functional diversity of Kv currents. This diversity is increased by their association with accessory proteins capable of modulating gating properties and assist trafficking and multimerization (4). Finally, modulation of Kv currents may also rely on posttranslational modifications such as glycosylation and phosphorylation of the channel proteins, which can affect their folding, their trafficking, or their functional activity.

Among Kv channels, Kv1.3 was the first channel reported to modulate cell proliferation in T cells (5). Since then, many other Kv channels (such as Kv1.1, Kv1.5, Kv3.4, Kv10, and Kv11.1) have been linked to migration and proliferation in numerous non-excitable tissues, including cancer cells, T-lymphocytes, endothelial cells, macrophages, leukocytes, and vascular smooth muscle cells (VSMCs) (1, 2, 6–9).

Kv1.3 channels have been described as modulators of cell proliferation in many different tissues, most notably T-cells and VSMCs, but also in several cancer cell types, macrophages, microglia, and oligodendrocyte progenitors (10–12). In fact, the pro-proliferative effect of Kv1.3 could be also reproduced by its overexpression in a heterologous system in cells that do not normally express the protein (13). However, although the contribution of the Kv1.3 channels to activation, migration, and proliferation seems to be well established, the mechanisms by which Kv1.3 expression modulates these processes are mostly unknown to date. Several mechanisms, which may not be mutually exclusive, have been proposed, including the interaction of Kv1.3 with integrin receptors (14–16), the impact of K^+ efflux through Kv1.3 channels on changes of resting E_M needed for cell cycle progression, or the modulation of intracellular calcium levels that could influence the phosphorylation state of several proliferation-related signaling processes (17, 18).

In addition to this role of Kv1.3 channels in cell proliferation, there is evidence of a reciprocal modulation, as certain mitogens induce Kv1.3 channel up-regulation (5, 19, 20). In this regard it is interesting to highlight the observed up-regulation of Kv1.3 channels upon stimulation with PDGF, basic FGF, or FBS and the simultaneous down-regulation of Kv1.5, another

* This work was supported by grants from the Ministerio de Economía y Competitividad (MINECO), Instituto de Salud Carlos III (RIC, RD12/0042/0006, Red Heracles), and Programa Estatal de Investigación (BFU2013-45867-R; to J. R. L.-L. and M. T. P.-G.), Fundación Ramón Areces (CIVP16A1843; to M. A. d l F.), and Consejería de Sanidad de la Junta de Castilla y León (BIO/VA21/15; to M. A. d l F.). The authors declare that they have no conflicts of interest with the contents of this article.

[1] Both authors contributed equally.

[2] A FPI-fellow of the Spanish Ministerio de Economía y Competitividad.

[3] A fellow of the Junta de Castilla y León.

[4] A fellow of Fundación Ramón Areces.

[5] Both are equal senior authors.

[6] To whom correspondence should be addressed: Departamento de Bioquímica y Biología Molecular y Fisiología, Universidad de Valladolid, Edificio IBGM, c/ Sanz y Forés s/n, 47003 Valladolid, Spain. Tel.: 34-983-184590; Fax: 34-983-184800; E-mail: tperez@ibgm.uva.es.

[7] The abbreviations used are: Kv channels, voltage-dependent potassium channels; E_M, membrane potential; VSMC, vascular smooth muscle cell; DPO, diphenyl phosphine oxide; EdU, 5-ethynyl-2′-deoxyuridine; EGFP, enhanced GFP; RFP, red fluorescent protein; ANOVA, analysis of variance; HSD, honest significant difference; MWW, Mann-Whitney-Wilcoxon.

Kv1 subfamily member (10, 11, 13, 19, 21, 22). This observation led us to hypothesize that the Kv1.3/Kv1.5 ratio could be a landmark to define VSMCs phenotype, as proliferation of VSMCs derived from different vascular beds in both mice and human associates with an expression switch from Kv1.5 to Kv1.3 (13, 22). Furthermore, in support of this hypothesis we have previously described that heterologous expression of Kv1.3 increased HEK cell proliferation, whereas Kv1.5 expression decreases basal HEK proliferation (13).

An important question regarding the mechanisms linking Kv1.3 expression to proliferation is whether this association depends on the ion-conducting properties of the channel (and hence of the feedback regulation of E_M (17) or not. There are previous studies demonstrating that the effects of several K channels on cell proliferation are not dependent on conducting properties of the channel proteins (13, 23, 24). In the first study we found that poreless Kv1.3 mutants can induce proliferation to the same extent that wild type channels, an effect that is lost in mutant voltage-insensitive channels or channels unable to localize to the plasma membrane. These results suggest that Kv1.3 proteins are docking sites that allow the activation of proliferative signaling cascades. In native VSMCs we found that PDGF-induced proliferation could be inhibited by either selective Kv1.3 blockers (Margatoxin or 5-(4-phenoxybutoxy)psoralen) or by blockers of MEK/ERK and PLCγ pathways, both effects being non-additive (22), which suggests a shared mechanism. However, the detailed description of the role of Kv1.3 channels modulating mitogen-induced signaling cascades awaits further characterization.

In this work we sought to explore in more detail the contribution of Kv1.3 channels to cell proliferation by addressing some of the questions raised above. First, on the basis of the opposite effects of Kv1.5 and Kv1.3 channels on HEK cell proliferation, we constructed chimeric Kv1.3/Kv1.5 channels to identify the molecular determinants involved in those effects. Our data pointed to the intracellular C-terminal domain of Kv1.3 as responsible for the increased proliferation rate. Next, we explored the contribution of individual residues within this C-terminal region by mutation to alanine of the eight predicted phosphorylation residues. This approach identified a short region in the C terminus (the YS segment) comprising two residues (Tyr-447 and Ser-459) whose mutation abolished Kv1.3-induced proliferation. The contribution of YS segment to Kv1.3-induced proliferation was confirmed by designing several mutant channels, including a C-terminal-truncated Kv1.3 channel retaining the YS segment and chimeric Kv1.5 channels harboring the YS segment at different positions within their C terminus. Second, we also identified one signaling pathway that could link Kv1.3 phosphorylation and proliferation, as genetic or pharmacological blockade of MEK/inhibited Kv1.3 induced proliferation and phosphotyrosine labeling of the channel. Finally, we observed that voltage-induced conformational changes of Kv1.3 channels are important for proliferation, regulating the accessibility of these tyrosine phosphorylation sites. Channel phosphorylation increased by maneuvers that facilitate the closed to open transition and was diminished in mutant channels that reside in the inactivated state.

Materials and Methods

HEK293 Cells Maintenance and Transfection—HEK293 cells were maintained in DMEM medium supplemented with 5% FBS, penicillin-streptomycin (100 units/ml each), 5 μg/ml Fungizone, and 2 mM L-glutamine at 37 °C in a 5% CO_2 humidified atmosphere. HEK cells were transiently transfected with 1 μg of DNA by using Lipofectamine™ 2000 or TransIT-X2® reagent (Mirrus). For siRNA experiments, HEK cells were cotransfected with 1 μg of DNA together with one or a mixture of siRNA at a final concentration of 5 nM. Transfection efficiency was quantified in each experiment by fluorescence microscopy (35–60%). Treatments with specific inhibitors (PD98059 20 μM, Tocris Bioscience) or with modified media were applied during 4 h before determinations.

Plasmids Construction—Full-length hKv1.5 and hKv1.3 were obtained from either cDNA or genomic uterine artery VSMC DNA (MagNA Pure Systems, Roche Applied Science) to generate C-terminal fusion proteins when subcloned into pEGFP-N1 (addgene) or pmCherry-N1 (Clontech), respectively: pEGFP-N1-hKv1.5 and pmCherry-N1-hKv1.3. Chimeric K5N3 and K5C3 channels were generated by PCR using *Phusion® Hot Start* High-Fidelity DNA Polymerase (Finnzymes). N or C termini from the Kv1.5 backbone were replaced by the corresponding domains of Kv1.3, creating the fusion proteins: pmCherry-N1-K5N3 and pEGFP-N1-K5C3. YS fragment is a 16-amino acid-residue fragment located at the proximal region of the C-terminal of Kv1.3 and containing residues Tyr-447 and Ser-459. The YS fragment was inserted within the hKv1.5 COOH terminus at two different positions, amino acid 532 (Kv1.5-YS^{532}) by overlap extension PCR or at the end of the C terminus (amino acid 613, Kv1.5-YS^{613}), by designing overlapping oligos. A truncated Kv1.3 containing the YS fragment and lacking C-terminal amino acids 461–523 (Kv1.3-YS) was also generated with overlapping oligos. Alanine substitutions were introduced at any of the potential phosphorylation residues Ser, Thr, and Tyr (predicted by NetPhos 2.0 Server) of Kv1.3 C terminus. With the exception of T439A that served as a control, all the selected residues were out of the Kv1.3-Kv1.5 consensus amino acid sequence. Mutagenesis was performed with the Stratagene QuikChange II site-directed mutagenesis kits using pmCherry-N1-hKv1.3 fusion protein as template. All constructs were sequence-verified.

Proliferation Assays—Once transfected, cells were counted with a hemocytometer and seeded at a density of 50,000 cells/well on 12-mm poly-lysine-coated coverslips. Proliferation was determined 24 h after seeding cells using a commercial kit (ClickiT® EdU Imaging Cell Proliferation Assay, Invitrogen) following previously described protocols (22). The percentage of cells at the S phase was quantified using 5-ethynyl-2′-deoxyuridine (EdU) incorporation for a 30-min period. Determinations were carried out in triplicate samples, and controls were included in all experiments.

qPCR Analysis of siRNA Efficiency—HEK cells were transfected with Ambion, Silencer® Select siRNAs. The siRNAs used were MAP2K1 (s11176 and s11168), MAP2K2 (s11170), and negative control (AM-4611). 48 h afer transfection total RNA was isolated using TRIzol reagent (Invitrogen), and mRNA lev-

els were determined by qPCR with Taqman® probes in a Rotor-Gene 3000 instrument (Corbett Research). Data were analyzed with the threshold cycle relative quantification method (ΔΔCt), normalized to an endogenous control (ribosomal protein L18). Taqman assays used were Hs00983247_g1 (MAP2K1) and Hs01673993_m1 (MAP2K2). The corresponding siRNAs reduced MAP2K1 mRNA by 10-fold (from 0.96 ± 0.08 to 0.1 ± 0.003) and MAP2K2 by 3-fold (from 1.05 ± 0.1 to 0.36 ± 0.6). No cross-reactivity was observed.

Apoptosis Assays—Apoptosis was detected by TUNEL method (*In Situ* Cell Death Detection kit, Roche Applied Science) 24 h after seeding transfected HEK293 cells. Experimental positive and negative controls were also performed.

Electrophysiological Studies—Ionic currents were recorded at room temperature using the whole-cell or the cell-attached configuration of the patch clamp technique as previously described (13, 19). For the whole cell experiments we used an internal solution (High-K^+i) containing (125 mM KCl, 4 mM $MgCl_2$, 10 mM HEPES, 10 mM EGTA, 5 mM MgATP (pH 7.2 with KOH)). The composition of the bath solution (Standard-e) was 141 mM NaCl, 4.7 mM KCl, 1.2 mM $MgCl_2$, 1.8 mM $CaCl_2$, 10 mM glucose, and 10 mM HEPES (pH 7.4 with NaOH). Whole-cell currents were recorded using an Axopatch 200 patch clamp amplifier, filtered at 2 kHz (−3 db, 4-pole Bessel filter) and sampled at 10 kHz. When leak subtraction was performed, an online P/4 protocol was used. Recordings were digitized with a Digidata 1200 A/D interface driven by CLAMPEX 8 software (Axon Instruments). Outward K^+ currents were elicited by depolarizing pulses from a holding potential of −80 mV to +40 mV applied in 10-s intervals. In some cells full current/voltage curves were constructed from potentials ranging from −60 to +100mV in 10-mV steps. Kv1.3 and Kv1.5 were defined by their sensitivity to the selective blockers 5-(4-phenoxybutoxy)psoralen (100 nM) and diphenyl phosphine oxide-1 (DPO; 1 μM), respectively.

Cell attached recordings were used for the kinetic characterization of the currents, with a pipette solution containing 120 mM NaCl, 30 mM KCl, 2 mM $CaCl_2$, and 10 mM HEPES (pH 7.4 with NaOH) and a bath solution (High-K^+_e) with 150 mM KCl, 0.5 mM $MgCl_2$, 10 mM HEPES, 1 mM EGTA (pH 7.2 with KOH). Currents were elicited by 500 ms depolarizing pulses to +40 mV from a holding potential of −80 mV. IV curves were constructed with 800-ms-depolarizing pulses from −80 to +100 mV in 20-mV steps applied every 10 s. Conductance curves were obtained from the amplitude of the fit to a mono-exponential function of the tail currents upon repolarization to −80 mV. After normalization to the maximal conductance (G_{max}) the data were fitted to a Boltzmann function to obtain the $V_{0.5}$ of activation and the slope of the curve. The steady-state inactivation was studied with a two-pulse protocol, in which a 200-ms pulse to +40 mV was preceded by a family 1.8-s depolarizing pulses from −100 to +40 mV in 20-mV intervals applied every 20 s. The peak current amplitude of the +40-mV pulse was normalized to the maximal amplitude (obtained with the −100-mV prepulse), plotted as a function of the prepulse potential, and fitted to a Boltzmann function. To determine the membrane potential in the cell-attached patch, we assumed that in the High-K^+_e there was no voltage difference across the cell membrane. This was confirmed with the measurement of the K^+_i from an instantaneous IV curve. 100-ms depolarizing prepulses to +60 mV were followed by repolarization to potentials from −100 to +60 mV. The IV curve obtained allowed determination of the reversal potential of the current and calculation of the K^+_i so that we could correct the estimated transmembrane potentials.

Immunocytochemistry—Transfected HEK293 cells were fixed with 3.7% paraformaldehyde 24 h after seeding and blocked in 2% of normal goat serum with PBS (nonpermeabilized cells) or Triton X-100 0.1% (permeabilized cells). Nonpermeabilized cells were incubated with anti-Kv1.3 or anti Kv1.5 extracellular primary antibodies (APC101 or APC150, Alomone Labs), whereas permeabilized cells were incubated with anti-Kv1.3 COOH (75-009, NeuroMab) or anti-Kv1.5 COOH (APC004, Alomone Labs), all at a final concentration of 1:50. Goat anti-rabbit 488 (A-11008, Molecular Probes), goat anti-rabbit 532 (A-11009, Molecular Probes), or goat anti-mouse 532 (A-11002, Molecular Probes) secondary antibodies were used at 1:1000. Hoechst 33342 (1:2000)-labeled nuclei and coverslips were mounted with Vectashield (Vector Laboratories). Photomicrographs were acquired with a LEICA SP5 confocal microscope using LAS software.

Image Analysis—Confocal images from non-permeabilized transfected HEK293 cells were used to assess the relative expression of Kv1.3 and Kv1.5 constructs at the plasma membrane. 63× (1.4NA) objectives were used to capture images and Z-stacks with a pinhole aperture of 1 airy unit (95.5 μm with our experimental settings) and a voxel size compatible with the Nyquist criterion. Images were binarized using a threshold that was automatically defined by Fiji software rsb.info.nih.gov). EGFP ($488_{ex}/507_{em}$) or mCherry fluorescence ($587_{ex}/610_{em}$) was taken as a measure of total expression of the fusion proteins (A_{Total}), whereas secondary antibody images, 532 ($531_{ex}/554_{em}$) or 488 ($495_{ex}/519_{em}$) defined the membrane area ($A_{Membrane}$). Both values were used to compute the % of membrane expression.

Immunoprecipitation—Transfected HEK293 cells incubated with the corresponding treatments were treated with 250 μM pervanadate during the last 5 min of incubation. Cell lysates collected in radioimmune precipitation assay buffer (150 mM NaCl, 50 mM Tris (pH 8), 1% Nonidet P-40, 0.2% sodium deoxycholate) with 1× protease inhibitor mixture (Roche Applied Science) and 1 mM phosphatase inhibitors NaF and Na_3VO_4 were incubated with RFP/GFP-Trap_A beads (ChromoTek) for 2–3 h and used for immunoblotting. They were separated by SDS-PAGE in 10% polyacrylamide gels and transferred to nitrocellulose membranes. Mouse monoclonal anti-phosphotyrosine antibody (clone 4G10, Millipore), rat monoclonal anti-RFP antibody (5F8, ChromoTek), rat monoclonal anti-GFP (3H9, ChromoTek), rabbit anti p-ERK1/2 (Cell Signaling 9101), and mouse monoclonal anti-β-actin (ab8226, Abcam) were used at a final concentration of 1:1,000 and incubated overnight at 4 °C. Secondary antibodies HRP-goat anti-mouse (Dako) HRP-goat anti-rat (Abcam), or HRP-goat anti-rabbit (Santa Cruz, sc-2301) were used at final concentration 1:20,000 for 1 h and developed with VersaDoc 4000 Image System (Bio-Rad) using chemiluminescence reagents (SuperSignal West Femto

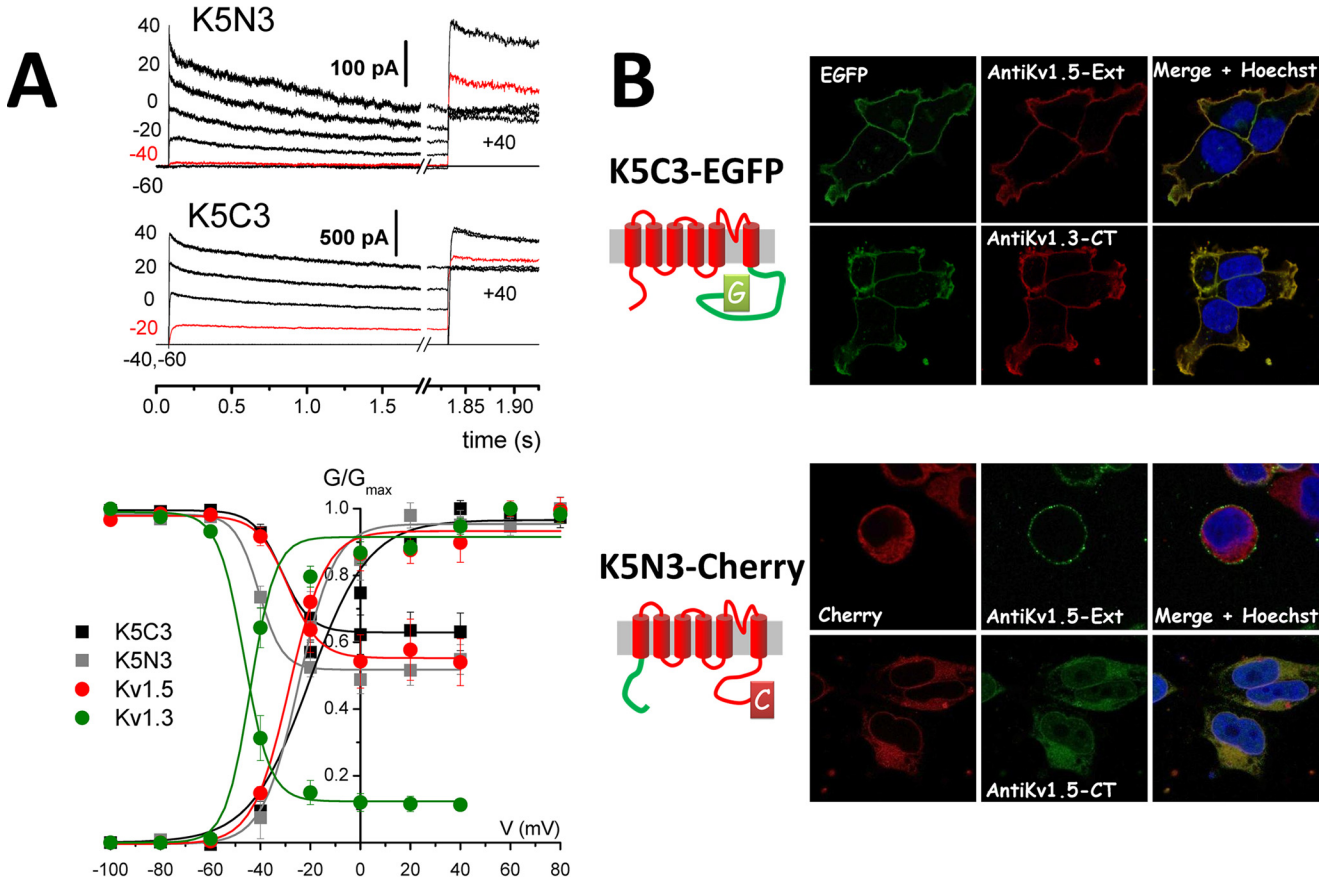

FIGURE 1. **Functional expression of K5N3 and K5C3 chimeras.** *A*, representative traces of K5N3 and K5C3 currents evoked by a steady-state inactivation protocol in transfected cells. A family of 1.8-s depolarizing pulses from −60 to +40 mV (as indicated in the *y* axis) was followed by a 200-ms depolarizing pulse to +40. The peak current amplitude in the prepulse was used to construct activation curves, whereas the amplitude of the pulse at +40 mV was plotted as a function of the voltage of the prepulse to create the inactivation curves. The trace elicited by the voltage closest to the inactivation $V_{0.5}$ is depicted in *red*. The *lower panel* shows average, normalized conductance-voltage relationships and Boltzmann fits for activation and inactivation obtained from Kv1.3-, Kv1.5-, K5C3-, and K5N3-transfected cells. Data are represented as the mean ± S.E. of 7–11 cells. *B*, confocal images obtained in HEK293 cells transfected with vectors expressing K5C3-EGFP and K5N3-Cherry chimeric vectors. The *left panels* show the fluorescence of the fusion protein, the *middle panels* show the antibody labeling, and the *right panels* show the merged images with Hoechst to see nuclear staining (*blue*). Membrane expression was determined in nonpermeabilized cells with an extracellular anti-Kv1.5 antibody (shown in *red* for K5C3 and in *green* for K5N3). Subcellular expression was determined in permeabilized cells by using antibodies against the cytoplasmic C terminus (*CT*), an anti-Kv1.3-CT antibody (*red*) and an anti-Kv1.5-CT antibody (*green*), respectively. Constructs are depicted on the *left schemes*.

Chemiluminescent Substrate, Pierce). The relative amount of protein was calculated by densitometric analysis of the bands using Fiji (Image J) software.

Data Analysis—Electrophysiological analyses were performed with both the CLAMPFIT subroutine of the PCLAMP software (Axon) and ORIGIN 7.5 software. Pooled data are expressed as the means ± S.E.

The composite data are expressed as the means ± S.E. Statistical analysis was performed using paired or unpaired test as appropriate. For pairwise comparison of normal distribution, Student's *t* test was used. For comparisons of several groups, one-way ANOVA was performed followed by a Shapiro-Wilk normality test of the fit of the residuals. In the case of normal distributions, comparisons among groups were performed with Tukey's honest significant difference (HSD) test. In the case of un-normal distributions (*i.e. p* value in the Shapiro-Wilk test of residuals <0.05), a Kruskal-Wallis one-way analysis of variance by ranks was used as a nonparametric method to test whether samples originate from the same distribution. When the null hypothesis was rejected, a pairwise Mann-Whitney-Wilcoxon (MWW) test with a Bonferroni correction was applied. In all cases, differences were considered to be significant when $p < 0.05$.

Results

The C-terminal Domain Contains the Molecular Determinants of Kv1.3-induced Proliferation—We constructed two chimeric channels (K5N3 and K5C3) using the backbone of Kv1.5 channels and substituting either the amino (K5N3) or the C-terminal (K5C3) intracellular domains with the corresponding regions of Kv1.3 channels. Both chimeras were constructed as fusion proteins with a fluorescent protein attached to the C terminus: EGFP for K5C3 and Cherry for K5N3. Upon expression, both chimeras formed functional channels with some mixed biophysical properties (Fig. 1*A* and Table 1); 1) current density was much larger for the K5C3 than for K5N3 channels; 2) inactivation time course and $V_{0.5}$ of activation were similar to Kv1.5 channels in both chimeras, and 3) $V_{0.5}$ of inactivation of K5N3 was similar to Kv1.3, whereas K5C3 was not different from Kv1.5. Differences in current density were related to the efficiency of trafficking to the plasma membrane as shown by

TABLE 1

Electrophysiological characterization of the amplitude and kinetics of the currents recorded from Kv1.3 and Kv1.5 channels and the mutants and chimeras

All data were obtained from cell-attached experiments. Data are the mean ± S.E. (*n*). Statistics were performed against the corresponding wild type channel (Kv1.3 for the four upper rows or Kv1.5 for the lower rows), and significant differences are depicted in bold. Pairwise comparison, *t* test.

Channel	Peak current + 40 mV	Inactivation at 800 ms	Activation		Inactivation	
			$V_{0.5}$	Slope	$V_{0.5}$	Slope
	pA	*%*	*mV*		*mV*	
Kv1.3	1501.88 ± 207.3 (10)	70.8 ± 2.3 (10)	−46.9 ± 2.8 (8)	6.2 ± 1 (8)	−46.6 ± 1.7 (6)	5 ± 0.5 (6)
Kv1.3-Y447A	1618.6 ± 283.4 (5)	62.1 ± 2.8 (5)	−50.2 ± 2.3 (5)	7 ± 2.7 (5)	−48.7 ± 1.8 (5)	3.6 ± 0.9 (5)
Kv1.3-S459A	2325.2 ± 709.4 (5)	79.3 ± 3.4 (5)	−41.3 ± 4.2 (5)	4.7 ± 1 (5)	−48.9 ± 7.8 (5)	3.3 ± 0.5 (5)
Kv1.3-YS	**508.5 ± 139.2[a] (9)**	75.8 ± 4.1 (9)	**−55.3 ± 2.8[b] (8)**	**3.3 ± 0.6[b] (8)**	−44.2 ± 2.6 (6)	3.9 ± 0.7 (6)
K5C3	1077.1 ± 288.2 (13)	38.9 ± 4.3 (13)	−20.4 ± 1.9 (11)	10.6 ± 1 (11)	−31 ± 2.2 (6)	5.3 ± 0.9 (6)
K5N3	**41.3 ± 6.1[b] (7)**	35 ± 3 (7)	−25.9 ± 1.5 (7)	5.3 ± 1 (7)	**−41.7 ± 1.4[a] (6)**	4.3 ± 0.8 (6)
K5N3+Kvβ2	170.7 ± 37.6 (8)	40.7 ± 4.2 (8)	**−39.6 ± 1.2[a] (6)**	6.6 ± 1.3 (6)	**−45.5 ± 1.2[c] (7)**	6.2 ± 1.3 (7)
Kv1.5-YS^{532}	241.6 ± 61.4 (8)	30.9 ± 3.7 (8)	**−14.8 ± 3.7[a] (8)**	**13.9 ± 1.5[a] (8)**	−25.1 ± 1.9 (5)	6.2 ± 0.7 (5)
Kv1.5-YS^{613}	252.6 ± 81.6 (10)	29.6 ± 5 (9)	−22.2 ± 2.3 (10)	10.7 ± 1.4 (10)	−30.2 ± 4.8 (7)	5.9 ± 1.3 (7)
Kv1.5	577.3 ± 234 (7)	37.7 ± 2.6 (6)	−27.7 ± 1.6 (7)	7.2 ± 0.8 (7)	−26.5 ± 3.1 (6)	6.8 ± 1.9 (6)

[a] $p < 0.01$.
[b] $p < 0.05$
[c] $p < 0.001$.

TABLE 2

Summary data of the surface expression of all Kv1.3 and Kv1.5 constructs

Data are the mean ± S.E. (*n*). Statistical differences with the corresponding wild type channel (Kv1.3 for the Kv1.3 constructs and Kv1.5 for Kv1.5 constructs) are indicated. For Kv1.3 constructs significant differences were obtained with one-way ANOVA followed by Tukey's HSD. For Kv1.5 channels, a nonparametric Kruskal-Wallis one-way ANOVA was used followed by a pairwise MWW test with Bonferroni correction. Significant differences are depicted in bold.

Kv1.3 constructs	% Cell surface expression	Kv1.5 constructs	% Cell surface expression
Kv1.3	39.82 ± 2.28 (23)	Kv1.5	37.72 ± 1.97 (40)
Kv1.3- T439A	43.31 ± 2.37 (11)	K5C3	**96.11 ± 4.01[a] (10)**
Kv1.3 Y447A	36.80 ± 4.78 (13)	K5N3	**21.11 ± 1.6[b] (25)**
Kv1.3-S459A	42.11 ± 4.81 (13)	K5N3 + Kvβ2	**27.32 ± 2.83[c] (20)**
Kv1.3-S470A	47.39 ± 3.26 (12)	Kv1.5-YS^{532}	44.75 ± 5.6 (18)
Kv1.3-S473A	46.51 ± 3.25 (11)	Kv1.5-YS^{613}	40.58 ± 4.4 (15)
Kv1.3-S475A	42.95 ± 4.31 (12)		
Kv1.3 Y477A	34.14 ± 2.55 (11)		
Kv1.3-T493A	39.97 ± 1.76 (22)		
Kv1.3-YS	**30.31 ± 3.3[c] (15)**		

[a] $p < 0.001$.
[b] $p < 0.01$
[c] $p < 0.05$.

immunocytochemical labeling of non-permeabilized cells with extracellular Kv1.5 antibody (Fig. 1*B* and Table 2). The fluorescence overlapping signals of the labeled antibody and the fusion proteins demonstrates that most K5C3 molecules localized to the cell surface, whereas a large amount of K5N3 was retained intracellularly and did not reach the plasma membrane.

The pharmacological profile of both chimeras resembles that of Kv1.5 channels (Fig. 2). Both mutants were sensitive to the Kv1.5-selective blocker DPO and did not respond to the selective Kv1.3 blocker 5-(4-phenoxybutoxy)psoralen (100 nM, data not shown). We tested proliferation after transient transfection of K5N3-, K5C3-, Kv1.3-, Kv1.5-, or EGFP-expressing plasmids. We observed that K5N3 inhibited proliferation to the same extent as Kv1.5, whereas K5C3 potentiated proliferation very much like Kv1.3 (Fig. 3*A*). These experiments suggest that the molecular determinants for the effect of the channels on cell proliferation are contained in their C-terminal domain. However, the reduced membrane expression (and hence the small current density) of K5N3 could be a potential caveat for our interpretation, as the low expression levels (and not the molecular structure of the chimera) could be altering proliferation. To test this possibility, HEK cells were co-transfected with K5N3 and an excess of Kvβ2.1 subunit, a chaperone subunit of Kv1 channels. This maneuver significantly increased the surface expression of the chimeric channels and, as previously described for both Kv1.5 and Kv1.3 (25, 26), induced a hyperpolarizing shift on the activation curve (Fig. 3*B*). However, despite the increased current density there were no significant changes on the effect on HEK cells proliferation (Fig. 3*C*).

Role of Individual Sites within the C-terminal Domain of Kv1.3 to the Proliferation Rate of HEK Cells—Our data suggest that the C-terminal domain of Kv1.3 channels was responsible for the channel effect on proliferation. To identify more precisely the amino acid residues involved in this effect, we mapped the phosphorylation sites within this region by generating eight mutants in which individual serines, tyrosines, or threonines were replaced by alanine (Fig. 4). Compared with wild type Kv1.3 channels we did not observe significant changes in any mutant in either their functional expression (studied with electrophysiological techniques) or their membrane trafficking (determined as above using an extracellular Kv1.3 antibody; Tables 1 and 2). Proliferation studies were carried out with the eight mutants always using Kv1.3 and cherry transfections as positive and negative controls, respectively. Our data (Fig. 4) shows that five of the point mutants (Y447A, S459A, S473A, S475A, Y477A) altered the pro-proliferative effect of Kv1.3 channel expression. Interestingly, three of them (Y447A, S459A, and Y477A) completely abolish the effect, as the proliferation in the presence of any of them was no different from control, cherry-transfected cells. Evaluation of the current density obtained with these transfectants (Fig. 4) showed no difference with the wild type Kv1.3 channels in all the mutants explored, in agreement with the co-localization studies (Table 2).

Confirmation of the Pivotal Role of Tyr-447 and Ser-459 Residues in Kv1.3-induced Proliferation—Modulation of Kv1.3 channel activity and kinetics in response to treatment with EGF or insulin has been shown to involve phosphorylation of tyrosine 477 but not of 447 (27). However, in our study point mutations to alanine of residues Tyr-447 and Ser-459 generated the two channel mutants that more efficiently abolished Kv1.3-induced proliferation. These residues are located at the proximal end of the Kv1.3 channel C terminus, in a region not previously identified as a conserved motif for interaction with growth fac-

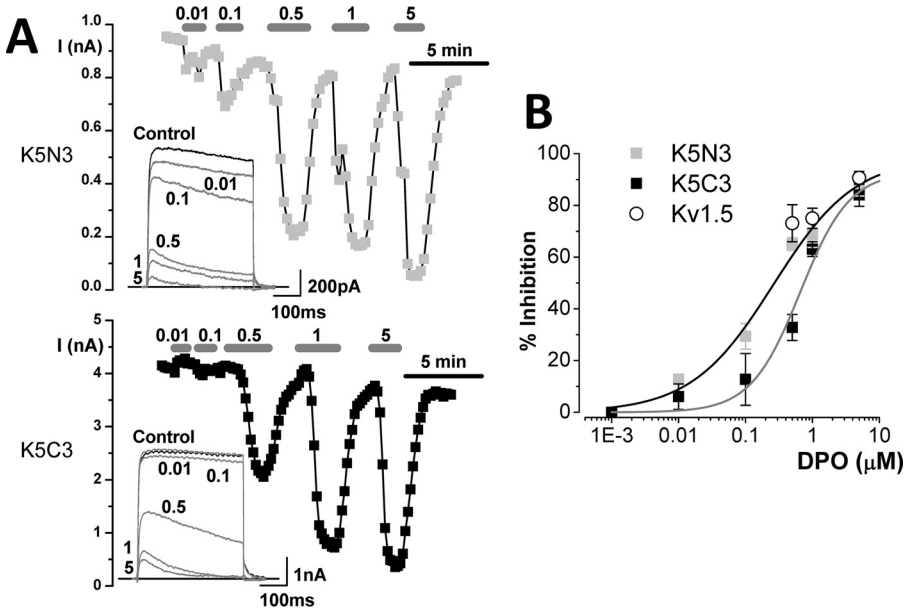

FIGURE 2. **Dose-response curves for the effect of DPO on K5N3 and K5C3 currents.** *A*, the plots show the current amplitude at the end of depolarizing pulses to +40 mV from a holding potential of −80 mV, applied every 10 s, from a HEK cell transfected with K5N3 (*upper graph*) or with K5C3 (*lower graph*). DPO was applied to the bath solution at the concentrations indicated (in μM) during the time marked. The *insets* show sample current traces at the different DPO concentrations. *B*, normalized dose-response curves obtained for the inhibitory effect of DPO on the current amplitude in both chimeric channels as well as in Kv1.5 (*open circles*). Each data point is the mean ± S.E. of 9–18 cells. The lines show the fit of the data from K5N3 and K5C3 channels to a Hill function (IC_{50} = 0.66 μM for K5C3 and 0.26 μM for K5N3).

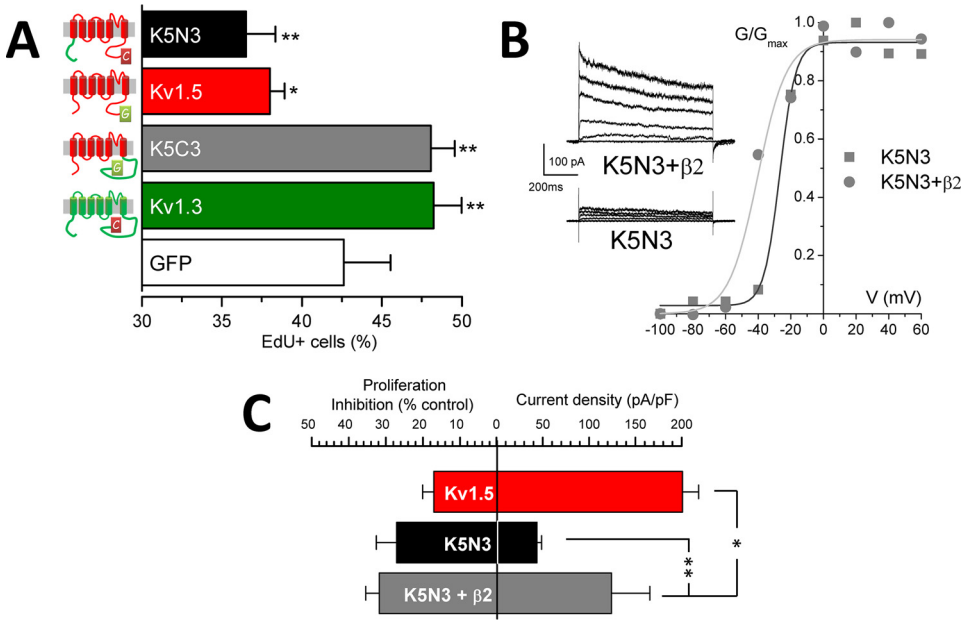

FIGURE 3. **Effects of K5N3 and K5C3 channels on HEK cell proliferation.** *A*, proliferation rate of HEK cell transfected with GFP-expressing vector (used as control) or with the indicated channels was determined by measuring the fraction of cells incorporating EdU reagent after 30 min of incubation in media with 5% FBS. Each *bar* is the mean ± S.E. n = 12–15. Data were from at least four different experiments. Comparisons were carried out with a one-way ANOVA and Tukey's HSD test as post hoc analysis, and significant differences with control and GFP-transfected cells are shown. *, $p < 0.05$; **, $p < 0.01$. *B*, representative examples of family of currents elicited by 500-ms depolarizing pulses from −80 to +60 mV in 20 mV from a HEK cell expressing K5N3 alone or together with the chaperone subunit Kvβ2.1. In addition to the increased current amplitude, there was a leftward shift in the voltage dependence of activation upon Kvβ2.1 coexpression. The data are representative of seven cells in each group. *C*, the changes in the current density of K5N3 channels do not modify their effect on proliferation. The plot shows the inhibition of proliferation (*left bars*; n = 4) and the current density at +40 mV (*right plot*; n = 8–15) from whole cell experiments of HEK293 expressing Kv1.5, K5N3, and K5N3+Kvβ2.1. Statistical differences from control (Kv1.5) were calculated with a Kruskal-Wallis test followed by a pairwise MWW with Bonferroni correction. *pF*, picofarads.

tor-associated kinases. We constructed some additional chimeric channels to confirm the contribution of this region (that we named the YS segment; Fig. 4) to the effect of Kv1.3 channels on proliferation. We created a truncated Kv1.3 channel with a short C-terminal domain comprising only the YS segment (Kv1.3-YS). Two additional chimeric channels were constructed by inserting this YS segment at two different positions into the Kv1.5 channel C terminus: either proximal in the equivalent location in Kv1.3 channels (after residue 532, Kv1.5-YS^{532}) or at the end of the protein (Kv1.5-YS^{613}). Both Kv1.5-

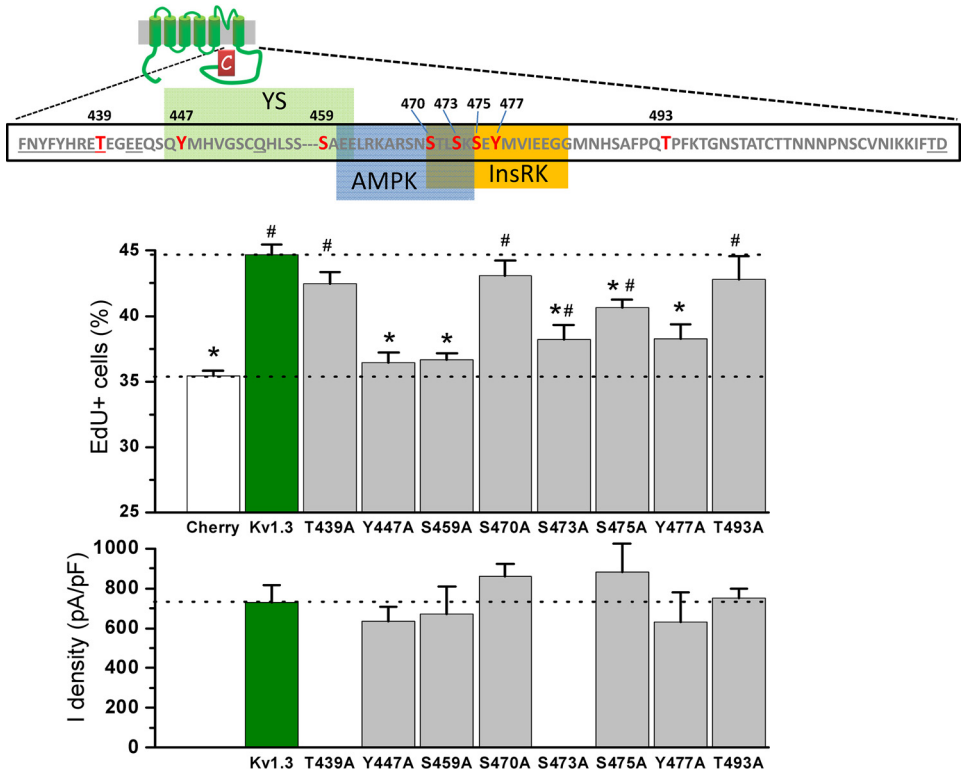

FIGURE 4. **Characterization of the effects on proliferation of Kv1.3 COOH terminus point mutants.** The schematic shows the position in the C terminus of Kv1.3 of the phosphorylatable residues (in *red*) that have been mutated to alanine. Also, AMP kinase and the insulin receptor kinase putative motifs are indicated as well as the YS segment. Conserved residues in the C terminus of Kv1.3 are *underlined*. The *upper panel* shows EdU incorporation assay of HEK293 cells transfected with each point mutant channels using Cherry and Kv1.3 expressing cells as controls. Each *bar* is the mean ± S.E. ($n = 6–20$ determinations from 3–7 different experiments). *, $p < 0.05$ compared with Kv1.3; #, $p < 0.05$ compared with Cherry, pairwise MWW with Bonferroni correction. The *lower plot* shows the current density at +40 mV obtained from whole-cell experiments ($n = 5–8$ cells).

YS^{532} and Kv1.5-YS^{613} show kinetic and pharmacological properties similar to Kv1.5 channels. Moreover, their trafficking did not show significant differences compared with wild type channels (Fig. 5*B*, Table 2). Meanwhile, Kv1.3-YS showed biophysical properties similar to Kv1.3 channels (Fig. 5*A*), albeit we observed some differences in their activation kinetics (Table 1) as well as a decreased membrane expression (Table 1 and 2). The impact on proliferation of these constructs is summarized in Fig. 5*C*. The truncated Kv1.3 channel (Kv1.3-YS) was still able to induce proliferation, although to a lesser degree than wild type Kv1.3. Interestingly, the Kv1.5-YS^{532} chimera increased proliferation similar to Kv1.3, whereas Kv1.5-YS^{613} behaved as Kv1.5 channels. These data indicated that the YS segment suffices to convert Kv1.5 channels into Kv1.3 channels with regard to their proliferative properties, but the environment in which the YS segment is inserted is relevant for this effect. In fact, all the chimeras containing the Kv1.3 YS segment located in the homologous region of Kv1.5 channels (the proximal end of C termini), have a stimulating effect on HEK proliferation (Fig. 5*D*) that is independent of the amount of current they can carry (or their membrane expression).

Identification of the Proliferation-activated Signaling Pathway Modulated by Kv1.3 Expression—The pro-proliferative role of native Kv1.3 channels in VSMCs is mediated by ERK1/2 signaling pathway, as selective blockers of Kv1.3 or selective blockers of the ERK1/2 cascade inhibited proliferation in a non-additive fashion (22). We have explored if this pathway could also be involved in the Kv1.3 induced proliferation in HEK cells. Treatment of HEK cells with the ERK1/2 blocker PD98059 (20 μM) was able to suppress Kv1.3-induced proliferation and had no effect in control cells (Cherry-transfected) or in cells transfected with the mutant channels Y447A and S459A (Fig. 6*A*). Genetic blockade of MEK1/2 by co-transfection of cherry or Kv1.3 constructs with a mixture of three MEK1/2 siRNAs fully reproduced the effects of PD98059 on HEK cells proliferation (Fig. 6*B*). These experiments suggest that the Kv1.3 effect on proliferation requires ERK1/2, and we hypothesize that either Tyr-447 or Ser-459 needs to be phosphorylated for Kv1.3 channels to induce proliferation. Immunoblots with anti-phosphotyrosine antibodies of Kv1.3 or Y447A-transfected HEK lysates after immunoprecipitation with anti-Cherry antibody support this hypothesis. In Kv1.3-transfected cells we show a clear phosphorylation signal of Kv1.3 that decreased after PD98059 treatment. There was a decreased basal phosphotyrosine content of Y447A-transfected cells compared with Kv1.3, and the treatment with the inhibitor did not have any effect (Fig. 6*C*). Besides, immunoprecipitation assays with anti-Cherry antibodies of Cherry- or Kv1.3-cherry-transfected cells demonstrated binding of pERK to the complexes containing Kv1.3 channels only upon treatment with phosphatase inhibitors, suggesting a brief, reversible interaction between them (Fig. 6*D*).

The correct location of Tyr-447 and Ser-459 within the channel protein seems to also be relevant for the effect on prolifer-

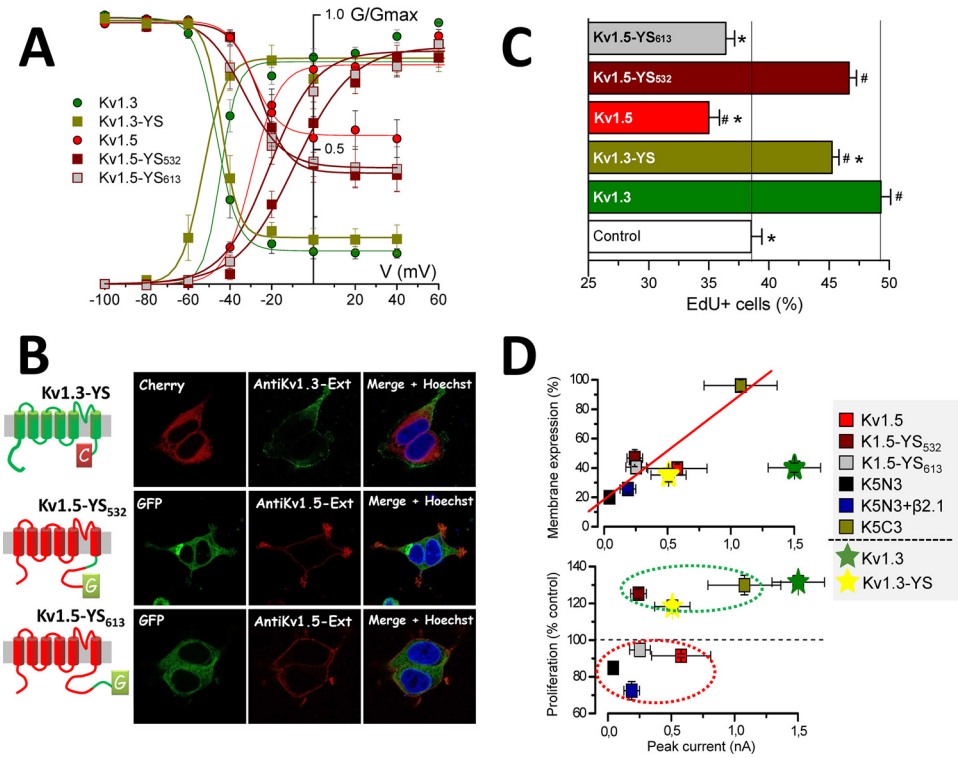

FIGURE 5. **Characterization of the Kv1.3 and Kv1.5 mutant channels containing the YS segment.** *A*, average normalized activation and inactivation curves are shown as conductance-voltage relationships for Kv1.3, Kv1.5, the truncated Kv1.3-YS channel, and the chimeras Kv1.5-YS^{532} and Kv1.5-YS^{613}. All datasets were fitted to Boltzmann functions. Each data point is the mean ± S.E. of 6–11 cells. *B*, confocal images of non-permeabilized cells transfected with Kv1.3-YS-Cherry, Kv1.5-YS^{532}-EGFP, and Kv1.5-YS^{613}-EGFP. An extracellular anti-Kv1.3 antibody was used to label Kv1.3-YS (*green*), whereas the extracellular anti-Kv1.5 antibody was used for Kv1.5-YS^{532} and Kv1.5-YS^{613} chimeras (*red*). Nuclei were stained by Hoechst (*blue*). *C*, proliferation rate of the indicated channels or GFP-transfected cells (control) was determined by measuring EdU incorporation. Significant differences when comparing to Kv1.3 (*) or to control (#) are indicated. Statistical analysis was performed with one-way ANOVA followed by a Tukey's HSD multiple comparison. Each *bar* is the average of 9–15 determinations from 5 different assays. *D*, the average peak current amplitude obtained in cell-attached experiments for Kv1.5 channels and all the Kv1.5 chimeras was plotted against the % of the channels expressed at the plasma membrane (*upper graph*) or their normalized effect on proliferation (taking 100% as the proliferation rate of GFP-transfected HEK cells, *lower graph*). The correlation between expression and current was fit to a linear regression curve ($y = 18.54 + 0.0066x$, $R^2 = 0.85$, $p = 0.008$), but there was no correlation between proliferation and current amplitude ($R^2 = 0.23$, $p = 0.19$).

ation (as illustrated with the differences between Kv1.5-YS^{532} and Kv1.5-YS^{613}). This could be attributed to conformational changes of the channel that expose these residues. Based on our previous data (13) we hypothesize that conformational changes in response to changes in E_M may be necessary to expose the identified phosphorylation sites in the YS segment. We were able to explore this hypothesis for the tyrosine residues by studying the effect of high K^+-induced depolarizations. Kv1.3-transfected cells were incubated with extracellular solutions containing 10, 20, and 60 mM K^+_e during 20 min. High K^+_e induced a significant increase of phosphotyrosine labeling of Kv1.3 channels at all the concentrations tested (Fig. 7*A*). The effect of depolarization on tyrosine phosphorylation was transient, returning to control values for incubations of 2–4 h in high K^+_e (Fig. 7*B*). In addition we found that the phosphotyrosine content is higher in Kv1.3WF channels, a poreless channel mutant, and decreased in the pore and gate double mutant Kv1.3 WF3x, which does not have voltage-gating transitions at resting E_M or in the Kv1.3 AYA mutant, a poreless channel that does not traffic to the plasma membrane (Fig. 7*C*). Strikingly, Kv1.3 WF3x and Kv1.3 AYA were not able to induce HEK cell proliferation, whereas Kv1.3WF had an effect similar to Kv1.3 channels (13).

Discussion

In this study we undertook the molecular dissection of the Kv1.3 channel and the parallel changes observed in HEK proliferation to conclude with an attractive hypothesis aimed to understand the role of ion channels in cell proliferation. The opposite effect on cell proliferation of two channels of the same subfamily (Kv1.3 and Kv1.5) has been of seminal importance for accomplishing our goals. This antithetical role has been described in different cell lineages, including VSMCs, oligodendrocyte progenitor cells, and microglia (10–13, 21). The fact that these antagonist effects on cell proliferation could still be observed upon heterologous expression of the channels represented an opportunity to explore the molecular mechanisms that associate the expression of these channels with the changes in the rate of proliferation. The data obtained from our analysis provided clear-cut results regarding the mechanisms by which Kv1.3 channel expression can facilitate cell proliferation.

All the chimeric and mutant channels were located at the plasma membrane. Two of them had a decreased functional expression (*i.e.* a decreased current density) compared with their corresponding wild type channels, namely Kv1.3-YS (compared with Kv1.3) and K5N3 (compared with Kv1.5). It has been reported that Kv1.3 channels harbor a di-acidic signal

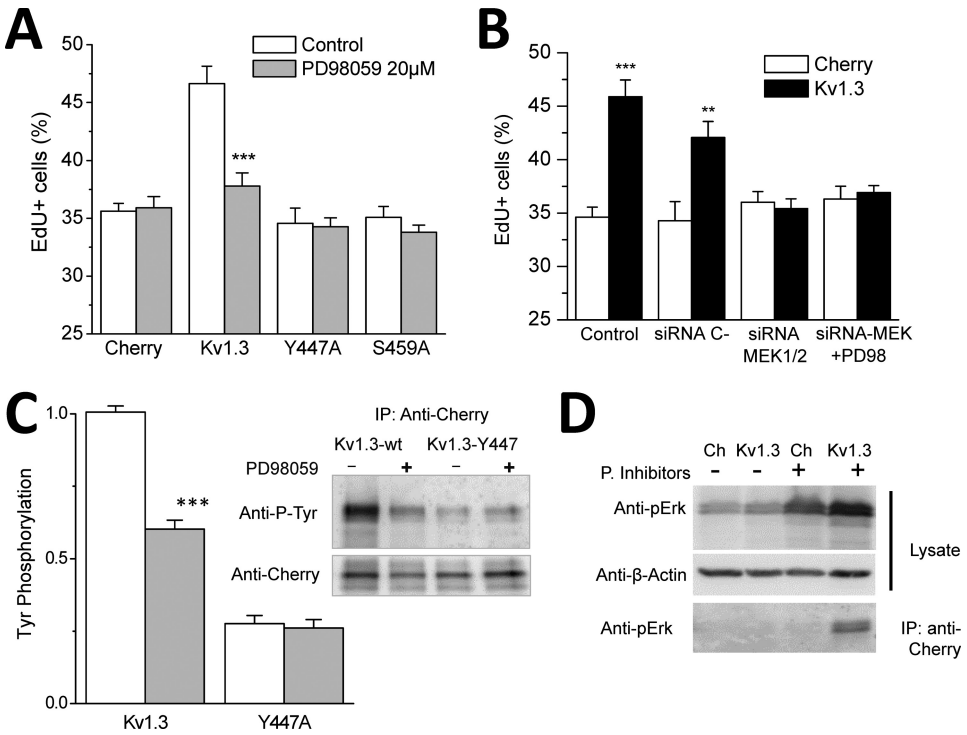

FIGURE 6. **MEK/ERK signaling pathway is involved in Kv1.3-induced proliferation.** *A*, proliferation rate of HEK293 cells transfected with an empty vector (Cherry), Kv1.3 channel, and the Y447A and S459A Kv1.3 mutant channels. Cells were kept in control media alone (*white bars*) or preincubated with PD98059 (20 μM) 4 h before the EdU incorporation assay. Data are the mean ± S.E. $n = 5–10$ determinations. ***, $p < 0.001$ when compared with its corresponding control (untreated), pairwise comparison with student *t* test. *B*, proliferation rate of HEK cells transfected with Cherry or Kv1.3 constructs alone (*Control*) or together with negative control siRNA or a mixture of 3 MEK1/2 siRNAs. The effect of PD98059 treatment in this latter group was also studied. Data are the mean ± S.E. of 5–12 determinations from at least three independent experiments. Student's *t* test was used to compare between Cherry- and Kv1.3-transfected cells in each group. *C*, the *bar plots* show the densitometric analysis obtained from 4–6 different experiments in which samples were immunoprecipitated (*IP*) with RFP-Trap_A beads and incubated with anti-phosphotyrosine (*P-Tyr*) antibody. The data were corrected for the labeling obtained with anti-cherry antibodies and normalized to the amount obtained for untreated Kv1.3-transfected cells. Pairwise Student's *t* test was used to compare between control and treated cells for each condition (Kv1.3 and Y447A). A representative immunoblot for Kv1.3- and Y447A-transfected cells incubated with (+) or without (−) PD98059 20 μM is shown (the target protein bands were ~84 kDa). *D*, representative immunoblot of cell lysates from Cherry (*Ch*)- or Kv1.3-transfected HEK cells with anti pERK1/2 antibody with or without treatment with phosphatase (P.) inhibitors. β-Acting was used as loading control. The *lower blot* shows anti-pERK1/2 labeling after immunoprecipitation of the same lysates with RFP-Trap.

(residues Glu-481/482 in human) essential for anterograde transport and surface expression (28) that is not conserved in Kv1.5 channels (see the schematic in Fig. 4). This could contribute to the decreased membrane expression of Kv1.3-YS and to the large increment both in current amplitude and membrane expression of K5C3 (see Tables 1 and 2). In this line, the reduced expression with K5N3 suggest that either the Kv1.3 N terminus has unique ER retention or retrograde trafficking signals or that the Kv1.5 N terminus has forward trafficking signals that are not present in Kv1.3.

Also, the changes in the biophysical properties of our mutant or chimeric constructs were in good agreement with the existing data regarding their molecular determinants. We confirm that the cytoplasmic N-terminal domains of Kv1.3 and Kv1.5 determine the voltage-dependent inactivation properties of the channels (29), and we reproduce the kinetic changes upon Kvβ2.1 coexpression (25, 26). Finally, the changes in the voltage dependence of activation observed in Kv1.3-YS and Kv1.5-YS^{532} are consistent with previous observations indicating that the coupling of the voltage sensor movement to operation of the gate mainly involves physical interactions of the S4-S5 linker with the intracellular end of S6 and/or the cytoplasmic "C-linker" region (30).

The contribution of Kv channels to cell proliferation has been associated with several mechanisms that do not need to be mutually exclusive such as their ability to sense and regulate E_M, their role in the control of cell volume, or their contribution to the regulation of calcium fluxes and intracellular calcium concentrations by means of the hyperpolarization of the E_M. Most of these mechanisms rely on the potassium gradients and focus on the potassium fluxes that generate the changes in cell volume or in resting E_M and do not consider the contribution of the ion channel molecule itself. However, non-conducting signaling roles of ion channels can also accompany these effects and in some cases are the main signal to induce proliferation. In these cases the cell cycle-associated oscillations of resting E_M may be mere byproducts of the changes in the expression or the conformational states of the ion channel (31). There are very few studies dissecting the contribution to the cell cycle of both conducting and non-conducting properties of ion channels, as this requires the use of genetic or pharmacological tools to selectively abolish ion permeation, although these evidences are clear for a few Kv channel molecules in different systems (32). Even more scarce is the information regarding the link(s) between voltage-dependent gating of Kv channels and cell cycle progression, although some clues are provided by the charac-

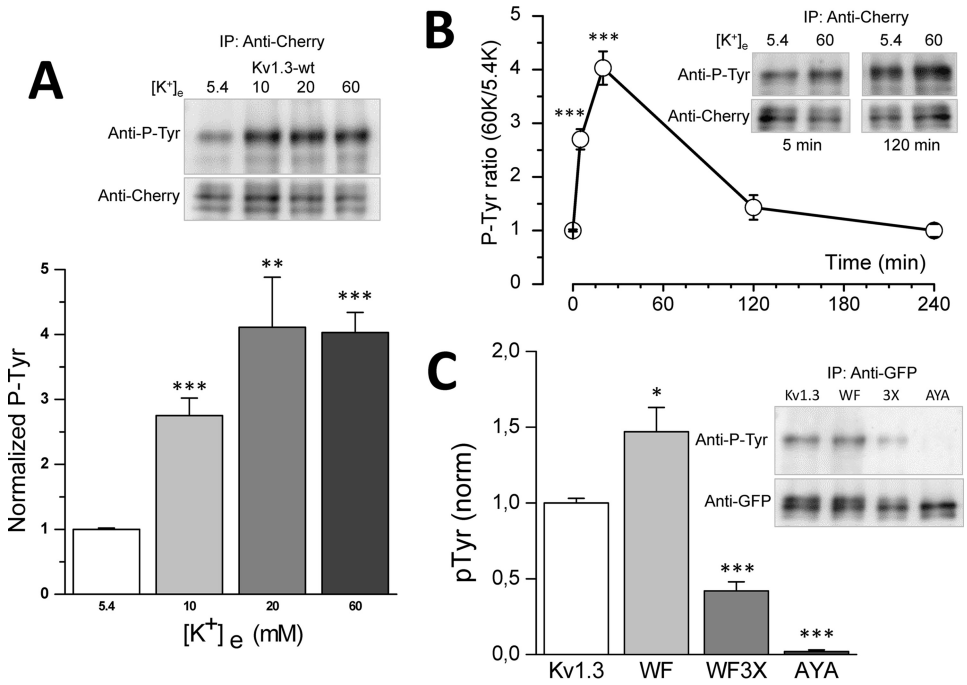

FIGURE 7. **Phosphotyrosine labeling of Kv1.3 channels is modulated by voltage-dependent transitions.** *A*, representative immunoblots and summary data from Kv1.3-transfected cells incubated with the indicated K^+_e solutions for 20 min before RFP-Trap immunoprecipitation (*IP*). p-Tyr labeling was corrected for anti-Cherry labeling and normalized to control data (cells incubated in 5.4 mM K^+). Statistical differences from control condition were established with a Tukey's HSD comparison after one-way ANOVA. *B*, time course of the effect of incubations with 60 mM K^+_e. At each time point, p-Tyr labeling is shown as the ratio of the 60/5.4 mM K^+_e signal. Each data point is the mean ± S.E. of 5–12 determinations from at least three independent experiments. Statistics were obtained with a MWW test pairwise comparison with Bonferroni correction and compared with the p-Tyr ratio at $t = 5$ min. *C*, immunoblot and densitometric average values of GFP-Trap-immunoprecipitated cells transfected with Kv1.3 or W389F-, WF3x-, and AYA Kv1.3-mutant channels. Data are normalized as above and are represented as the mean ± S.E. of 3–5 different experiments. Significant differences with Kv1.3 wild type channels were estimated with pairwise Student's *t* tests. *, $p < 0.05$; **, $p < 0.01$; ***, $p < 0.001$.

terization of the proteins associated with Kv channels in the macromolecular complexes (33, 34). In the case of Kv1.3 channels, these proteins include growth factor receptors (35) and cytoskeleton-associated molecules (15, 36). However, the interactions within these macromolecular complexes or the relationship between ion fluxes through the channels and the signaling cascades leading to proliferation awaits further characterization.

Our previous work with Kv1.3 mutant channels lacking either the pore or the voltage-gating mechanisms indicated that the ability of Kv1.3 channels to sense the voltage was essential for its role in facilitating proliferation, as only poreless channels with normal gating behavior were as effective as wild type Kv1.3 channels. We speculate that changes in resting E_M that contribute to cell cycle progression could be sensed and transduced through Kv1.3 channels. The requirement of Kv1.3 channels (and not a closely related Kv1 subfamily member such as Kv1.5) for the potentiation of proliferation indicates that either the Kv1.3 channel itself or other closely associated molecules must be targets/effectors in the proliferation signaling pathway. We postulated the existence of specific docking sites within the channel molecule whose exposure to proliferative stimulus is regulated by voltage-dependent conformational changes and potentiate cell proliferation. The results presented here support this hypothesis, providing some additional information regarding the molecular identification of these docking sites, the nature of the interacting molecules, and the mechanisms involved. We found that Kv1.3-induced proliferation of HEK cells can be fully abolished by three point mutations that eliminate three phosphorylation sites at the C-terminal domain. Moreover, we demonstrate that at least for one of these residues (Tyr-447) potentiation of proliferation is mediated by its phosphorylation and is dependent of an intact MEK/ERK signaling pathway (Fig. 6, *A* and *C*). Finally, our results with the chimeric channels containing the YS segment suggest that the location of this domain within the channel molecule also determines its ability to enhance proliferation. We speculate that the exposure of this region for being phosphorylated requires a conformational change of the molecule; differences in phosphotyrosine labeling of Kv1.3 channels in the presence of high K^+_e suggests that voltage-dependent transitions from closed to open state could represent this conformational change. Resting E_M of HEK cells changes from a mean value of −15 mV in mock-transfected (or Kv1.3WF-transfected) cells to −43 mV in Kv1.3-transfected cells (13). Interestingly, phosphorylation of Kv1.3WF is significantly higher than Kv1.3, as expected if we take into account that Kv1.3WF-transfected cells are more depolarized. Increasing K^+_e from 5.4 to 10, 20, or 60 mM depolarizes the cells to E_M values $> V_{0.5}$ of activation of the channel (−38, −30, and −14 mV, respectively), and in agreement with that we found increased Kv1.3 phosphorylation in the three conditions. Also, the requirement of a closed to open transition can explain the increased Tyr phosphorylation of Kv1.3WF (that shows normal gating currents) and the absence of Tyr phosphorylation of the pore and gating double mutant Kv1.3WF-3x (13). The contribution of phosphorylation of

Kv1.3 serine residues could not be determined with a similar approach. Unlike phosphotyrosines, which have a very specific epitope, there are not single antibodies that will recognize all or most phosphoserines independently of the surrounding amino acid sequence, and we failed to show phosphoserine labeling of Kv1.3 using several different experimental procedures. However, the physical association of pERK with the complexes containing Kv1.3 channels (Fig. 6*D*) could provide an indirect argument supporting a role for serine residues in proliferation signaling pathways, as ERKs substrates are phosphorylated in Ser/Thr residues.

Overall, our data suggest that the molecular nature of the voltage sensor that activates the signaling pathway facilitating proliferation is relevant. The effect on proliferation is lost when the channel is not able to sense the voltage and is increased when the voltage-dependent transitions are facilitated. However, the changes in E_M are not sufficient to promote proliferation, as illustrated by the overexpression of Kv1.5 channels, which promotes a similar hyperpolarization (13) but in the absence of the specific domains is not able to induce proliferation (in fact it has the opposite effect). These data open interesting questions to identify the signaling pathways by which Kv1.3 channels (and not Kv1.5 channels) potentiate cell proliferation in several native systems. The contribution of Kv1.3 channels to cell proliferation in these systems can be related to their role as effectors of the cell cycle machinery, participating in the regulation of signaling cascades via protein-protein interactions. The identification of these signaling cascades and of the molecules involved in this non-canonical function of Kv channels will provide a better understanding of these processes and will pave the way for the development of new, more specific therapies based on ion channels for controlling cell proliferation.

Author Contributions—P. C., M. A. F., M. T. P.-G., and J. R. L.-L. designed the experiments. L. J.-P., R. T.-M., and M. A. F. designed and performed mutant channel expression. L. J.-P., A. S.-H., E. A., and P. C. performed immunocytochemistry and immunoprecipitation, confocal studies, and proliferation assays. M. T. P.-G. and I. A.-M. performed electrophysiological experiments. L. J.-P., I. A.-M., P. C., J. R. L.-L., and M. T. P.-G. analyzed the data. L. J.-P., PC, M. T. P.-G., and J. R. L.-L. wrote the manuscript.

Acknowledgments—We thank Luis A. García-Escudero for help with statistical analysis and Henar Albertos for confocal images analysis.

References

1. Pardo, L. A. (2004) Voltage-gated potassium channels in cell proliferation. *Physiology* **19,** 285–292
2. Wulff, H., Castle, N. A., and Pardo, L. A. (2009) Voltage-gated potassium channels as therapeutic targets. *Nat. Rev. Drug. Discov.* **8,** 982–1001
3. Chandy, K. G., Wulff, H., Beeton, C., Pennington, M., Gutman, G. A., and Cahalan, M. D. (2004) K^+ channels as targets for specific immunomodulation. *Trends Pharmacol. Sci.* **25,** 280–289
4. Coetzee, W. A., Amarillo, Y., Chiu, J., Chow, A., Lau, D., McCormack, T., Moreno, H., Nadal, M. S., Ozaita, A., Pountney, D., Saganich, M., Vega-Saenz de Miera, E., and Rudy, B. (1999) Molecular diversity of K^+ channels. *Ann. N.Y. Acad. Sci.* **868,** 233–285
5. DeCoursey, T. E., Chandy, K. G., Gupta, S., and Cahalan, M. D. (1984) Voltage-gated K^+ channels in human lymphocyte-T: a role in mitogenesis. *Nature* **307,** 465–468
6. Erdogan, A., Schaefer, C. A., Schaefer, M., Luedders, D. W., Stockhausen, F., Abdallah, Y., Schaefer, C., Most, A. K., Tillmanns, H., Piper, H. M., and Kuhlmann, C. R. (2005) Margatoxin inhibits VEGF-induced hyperpolarization, proliferation, and nitric oxide production of human endothelial cells. *J. Vasc. Res.* **42,** 368–376
7. Miguel-Velado, E., Moreno-Domínguez, A., Colinas, O., Cidad, P., Heras, M., Pérez-García, M. T., and López-López, J. R. (2005) Contribution of Kv channels to phenotypic remodeling of human uterine artery smooth muscle cells. *Circ. Res.* **97,** 1280–1287
8. Cidad, P., Moreno-Domínguez, A., Novensá, L., Roqué, M., Barquín, L., Heras, M., Pérez-García, M. T., and López-López, J. R. (2010) Characterization of ion channels involved in the proliferative response of femoral artery smooth muscle cells. *Arterioscler. Thromb. Vasc. Biol.* **30,** 1203–1211
9. Beeton, C., Wulff, H., Standifer, N. E., Azam, P., Mullen, K. M., Pennington, M. W., Kolski-Andreaco, A., Wei, E., Grino, A., Counts, D. R., Wang, P. H., LeeHealey, C. J., S Andrews, B., Sankaranarayanan, A., Homerick, D., Roeck, W. W., Tehranzadeh, J., Stanhope, K. L., Zimin, P., Havel, P. J., Griffey, S., Knaus, H. G., Nepom, G. T., Gutman, G. A., Calabresi, P. A., and Chandy, K. G. (2006) Kv1.3 channels are a therapeutic target for T cell-mediated autoimmune diseases. *Proc. Natl. Acad. Sci. U.S.A.* **103,** 17414–17419
10. Kotecha, S. A., and Schlichter, L. C. (1999) Switch in endogenous hippocampal microglia and a role in proliferation. *J. Neurosci.* **19,** 10680–10693
11. Chittajallu, R., Chen, Y., Wang, H., Yuan, X., Ghiani, C. A., Heckman, T., McBain, C. J., and Gallo, V. (2002) Regulation of Kv1 subunit expression in oligodendrocyte progenitor cells and their role in G_1/S phase progression of the cell cycle. *Proc. Natl. Acad. Sci. U.S.A.* **99,** 2350–2355
12. Villalonga, N., David, M., Bielanska, J., Vicente, R., Comes, N., Valenzuela, C., and Felipe, A. (2010) Immunomodulation of voltage-dependent K^+ channels in macrophages: molecular and biophysical consequences. *J. Gen. Physiol.* **135,** 135–147
13. Cidad, P., Jiménez-Pérez, L., García-Arribas, D., Miguel-Velado, E., Tajada, S., Ruiz-McDavitt, C., López-López, J. R., and Pérez-García, M. T. (2012) Kv1.3 channels can modulate cell proliferation during phenotypic switch by an ion-flux independent mechanism. *Arterioscler. Thromb. Vasc. Biol.* **32,** 1299–1307
14. Levite, M., Cahalon, L., Peretz, A., Hershkoviz, R., Sobko, A., Ariel, A., Desai, R., Attali, B., and Lider, O. (2000) Extracellular K^+ and opening of voltage-gated potassium channels activate T cell integrin function: physical and functional association between Kv1.3 channels and β1 integrins. *J. Exp. Med.* **191,** 1167–1176
15. Artym, V. V., and Petty, H. R. (2002) Molecular proximity of Kv1.3 voltage-gated potassium channels and β1-integrins on the plasma membrane of melanoma cells: effects of cell adherence and channel blockers. *J. Gen. Physiol.* **120,** 29–37
16. Welschoff, J., Matthey, M., and Wenzel, D. (2014) RGD peptides induce relaxation of pulmonary arteries and airways via β3-integrins. *FASEB J.* **28,** 2281–2292
17. Hu, L., Gocke, A. R., Knapp, E., Rosenzweig, J. M., Grishkan, I. V., Baxi, E. G., Zhang, H., Margolick, J. B., Whartenby, K. A., and Calabresi, P. A. (2012) Functional blockade of the voltage-gated potassium channel Kv1.3 mediates reversion of t effector to central memory lymphocytes through SMAD3/p21cip1 signaling. *J. Biol. Chem.* **287,** 1261–1268
18. Robbins, J. R., Lee, S. M., Filipovich, A. H., Szigligeti, P., Neumeier, L., Petrovic, M., and Conforti, L. (2005) Hypoxia modulates early events in T cell receptor-mediated activation in human T lymphocytes via Kv1.3 channels. *J. Physiol.* **564,** 131–143
19. Colley, B. S., Biju, K. C., Visegrady, A., Campbell, S., and Fadool, D. A. (2007) Neurotrophin B receptor kinase increases Kv subfamily member 1.3 (Kv1.3) ion channel half-life and surface expression. *Neuroscience* **144,** 531–546
20. Lang, F., and Shumilina, E. (2013) Regulation of ion channels by the serum- and glucocorticoid-inducible kinase SGK1. *FASEB J.* **27,** 3–12
21. Vautier, F., Belachew, S., Chittajallu, R., and Gallo, V. (2004) Shaker-type potassium channel subunits differentially control oligodendrocyte pro-

genitor proliferation. *Glia* **48,** 337–345
22. Cidad, P., Miguel-Velado, E., Ruiz-McDavitt, C., Alonso, E., Jiménez-Pérez, L., Asuaje, A., Carmona, Y., García-Arribas, D., López, J., Marroquín, Y., Fernández, M., Roqué, M., Pérez-García, M. T., and López-López, J. R. (2015) Kv1.3 channels modulate human vascular smooth muscle cells proliferation independently of mTOR signaling pathway. *Pflugers Arch.* **467,** 1711–1722
23. Hegle, A. P., Marble, D. D., and Wilson, G. F. (2006) A voltage-driven switch for ion-independent signaling by ether-a-go-go K^+ channels. *Proc. Natl. Acad. Sci. U.S.A.* **103,** 2886–2891
24. Millership, J. E., Devor, D. C., Hamilton, K. L., Balut, C. M., Bruce, J. I., and Fearon, I. M. (2011) Calcium-activated K^+ channels increase cell proliferation independent of K^+ conductance. *Am. J. Physiol. Cell Physiol.* **300,** C792–C802
25. Uebele, V. N., England, S. K., Chaudhary, A., Tamkun, M. M., and Snyders, D. J. (1996) Functional differences in Kv1.5 currents expressed in mammalian cell lines are due to the presence of endogenous Kv β 2.1 subunits. *J. Biol. Chem.* **271,** 2406–2412
26. McCormack, T., McCormack, K., Nadal, M. S., Vieira, E., Ozaita, A., and Rudy, B. (1999) The effects of Shaker β-subunits on the human lymphocyte K^+ channel Kv1.3. *J. Biol. Chem.* **274,** 20123–20126
27. Bowlby, M. R., Fadool, D. A., Holmes, T. C., and Levitan, I. B. (1997) Modulation of the Kv1,3 potassium channel by receptor tyrosine kinases. *J. Gen. Physiol.* **110,** 601–610
28. Martínez-Mármol, R., Pérez-Verdaguer, M., Roig, S. R., Vallejo-Gracia, A., Gotsi, P., Serrano-Albarrás, A., Bahamonde, M. I., Ferrer-Montiel, A., Fernández-Ballester, G., Comes, N., and Felipe, A. (2013) A non-canonical di-acidic signal at the C-terminus of Kv1.3 determines anterograde trafficking and surface expression. *J. Cell Sci.* **126,** 5681–5691
29. Hoshi, T., Zagotta, W. N., and Aldrich, R. W. (1990) Biophysical and molecular mechanisms of Shaker potassium channel inactivation. *Science* **250,** 533–538
30. Barros, F., Domínguez, P., and de la Peña, P. (2012) Cytoplasmic domains and voltage-dependent potassium channel gating. *Front. Pharmacol.* **3,** 49
31. Becchetti, A. (2011) Ion channels and transporters in cancer. 1. Ion channels and cell proliferation in cancer. *Am. J. Physiol. Cell Physiol.* **301,** C255–C265
32. Urrego, D., Tomczak, A. P., Zahed, F., Stühmer, W., and Pardo, L. A. (2014) Potassium channels in cell cycle and cell proliferation. *Philos. Trans. R. Soc. Lond. B. Biol. Sci.* **369,** 20130094
33. Lee, A., Fakler, B., Kaczmarek, L. K., and Isom, L. L. (2014) More than a pore: ion channel signaling complexes. *J. Neurosci.* **34,** 15159–15169
34. Kaczmarek, L. K. (2006) Non-conducting functions of voltage-gated ion channels. *Nat. Rev. Neurosci.* **7,** 761–771
35. Fadool, D. A., Tucker, K., Perkins, R., Fasciani, G., Thompson, R. N., Parsons, A. D., Overton, J. M., Koni, P. A., Flavell, R. A., and Kaczmarek, L. K. (2004) Kv1.3 channel gene-targeted deletion produces "Super-Smeller Mice" with altered glomeruli, interacting scaffolding proteins, and biophysics. *Neuron* **41,** 389–404
36. Hajdu, P., Martin, G. V., Chimote, A. A., Szilagyi, O., Takimoto, K., and Conforti, L. (2015) The C terminus SH3-binding domain of Kv1.3 is required for the actin-mediated immobilization of the channel via cortactin. *Mol. Biol. Cell* **26,** 1640–1651